Ollscoil na Gaillimhe
University of Galway

Web geometry optimisation of novel latticed LVL-webbed timber I-joists

Title	Web geometry optimisation of novel latticed LVL-webbed timber I-joists
Author(s)	Harte, Annette M.;Baylor, Gordon;O'Ceallaigh, Conan
Publication Date	2022-12-02
Publisher	Elsevier
Repository DOI	doi:10.1016/j.istruc.2022.11.059

Web Geometry Optimisation of Novel Latticed LVL-Webbed Timber I-joists

Annette M. Harte, Gordon Baylor, Conan O'Ceallaigh
College of Science & Engineering & Ryan Institute, University of Galway, University Rd., Galway, Ireland.
Email: conan.oceallaigh@nuigalway.ie

ABSTRACT: This paper presents the finite element analysis of novel composite timber I-joists with curved latticed webs. The flanges of the joists were made from Norway Spruce whilst the curved latticed webs were made from laminated veneer lumber (LVL). The I-joists are analysed using the finite element method (FEM) with the component materials modelled as linear elastic orthotropic materials in both tension and compression. Good correlation was found between the experimental test results and the FE simulations when utilising material properties based on experimental investigation. The validated FE model was shown to reasonably predict the load-displacement behaviour and was used to assess the stress distributions within the novel I-joist and particularly in the latticed LVL web. The developed FE model provides a useful tool to further analyse and optimise the design. A geometric parameter study was carried out to enhance the structural performance of the novel I-joists by altering the geometry of the latticed web components and an optimised geometry is presented.

KEY WORDS: Engineered wood products, I-joist, Load-displacement behaviour, LVL, Timber structures; Finite element; Parameter study; Optimisation.

1 INTRODUCTION

The structurally engineered timber I-joist was successfully introduced into the construction market in the 1970s as an alternative to larger-dimension solid sawn timber. Compared to solid sawn timber elements, I-joists comprising timber flanges and a web can be a more efficient structural form and result in more efficient use of the material [1–3]. Additionally, they have the advantage of greater dimensional stability and lower variability in their structural performance when compared to solid timber elements [1,4]. They are one of the most commonly used Engineered Wood Products (EWPs) and have been extensively used in Europe and North America in both residential and commercial buildings for floor and roof applications e.g., suspended intermediate floors, suspended ground floors, purlins and rafters. The flanges are typically made from solid timber or laminated veneer lumber (LVL) and the web is often made from OSB, plywood or particleboard [2,3] but alternative materials have also been examined [5–7].

Openings are often incorporated in the webs of I-joists to allow services to pass through. By accommodating services within the depth of the floors, the overall structural depth can be reduced, or greater headroom provided. However, the presence of openings makes the stress distributions in the web more complicated and, depending on the configuration of the openings, can reduce the load-carrying capability of the joist [8–12]. Product manufacturers produce design guidance documentation to specify

Final Draft

permitted web hole requirements, which are generally restricted to circular or rectangular openings, and limits are provided on the dimensions of the openings as well as restricting the positioning of openings to low shear areas [13].

This study addresses the concept of a timber I-joist with a curved latticed LVL web, an example of which can be seen in **Fig. 1**. The web is manufactured using a process which is typically used in curved furniture applications. The concept of using curved lattice LVL components is unique in its application here in a structural timber member. The resulting shape provides a series of openings along the entire span, which provide flexibility in the routing of services at the construction stage through the web, and the rerouting of services during building retrofit. The novel lattice LVL-webbed I-joist has been the subject of an experimental study carried out by Harte et al. [14] whereby the structural behaviour of two different depths was evaluated. Further work is required to gain a better understanding of their behaviour and to optimise the design. These lattice LVL webbed joists are highly indeterminate structures, which are not well suited to simple methods of analysis. For this reason, the Finite Element (FE) method is used to model the behaviour of the I-joists. This paper describes a three-dimensional finite element model, which has been developed to model the structural performance of this novel latticed LVL webbed timber I-joist. The model is validated using experimental data and is then used in a parameter study which seeks to determine the influence on the structural response of a number of geometric characteristics of the latticed LVL web component. From this study, the optimum design parameters are selected.

Fig. 1. Manufactured latticed LVL-webbed I-joist

2 LITERATURE REVIEW

To date, while there are only a limited number of studies performed on timber I-joists, a large body of research exists on the structural behaviour of steel I-beams with different types of openings [15–21]. Experimental studies have identified a number of different failure modes associated with these joists including excessive stresses in the tee-sections above and below openings, failure of the web between two adjacent openings, web-buckling, and the formation of plastic hinges in the tee-sections above and below the openings resulting in a ‘Vierendeel’ type mechanism. It is generally expected that the shape of the web openings is critical in the structural behaviour of sections, and has been shown to be influential on the yield behaviour of such members, and also the mode of failure [15]. By extension, the presence of large web openings may also have a severe penalty on the load-carrying capacity of members [17].

Several authors have reported on the experimental testing and numerical modelling of timber I-joists with circular, rectangular or hexagonal web openings [8,10,11,22–28]. For the most part, these studies consider single openings or pairs of openings. Zhu

Final Draft

et al. [8] developed a three-dimensional non-linear finite element model for OSB-webbed timber I-joists with a single circular or square web opening. Additionally, joists with pairs of openings with different spacing were examined and critical distances where interactions adversely influenced the structural behaviour were identified. Tension failure of the OSB was defined using the Tsai-Hill failure criterion and the model predictions compared well with the results of experimental testing, which showed that circular openings performed better in terms of structural performance than square openings which were subject to the stress concentration at the corner of the square opening.

Morrissey et al. [11] undertook a series of tests on 38 commercial timber I-joists of two different depths (241 mm and 302 mm deep) to determine the effects of circular and square openings and also to examine retrofitting to reinforce the openings. Finite element modelling was also undertaken to gain a better understanding of the load-displacement behaviour, stress distributions and the failure mechanisms involved. The flange material was modelled as a linear elastic orthotropic material and the OSB web material was treated as a planar isotropic material. The numerically predicted service load deflections were between 97 and 114% of the experimental values for the 241 mm deep joists and between 85% and 111% of the measured deflections for the 302 mm deep joists.

Baylor and Harte [23] investigated the behaviour of composite timber I-joists using FE analysis. The OSB webs of the joists had hexagonal holes which resulted from the castellation manufacturing process. The component materials were modelled as linear orthotropic elastic materials in both tension and compression. Good correlation was obtained between the FE models and physical test data for nine 241 mm deep joists and eight 305 mm deep joists. There was an increase of 16.1% and 15.2% in the mid-span vertical displacement of the 241 mm and 305 mm I-joists, respectively due to web openings.

As far as the authors of the current work are aware, the only study to publish experimental results for latticed LVL web timber I-joists is Harte et al. [14]. The experimental program performed by Harte et al. [14] involved experimental tests on 241 mm and 305 mm deep I-joists with latticed LVL webs subjected to four-point bending loads. The load-deflection response, failure loads, and failure modes were recorded. The load-deflection response was found to be linear to failure in 21 of the 24 I-joists tested. For the remaining 3 I-joists, the load-deflection response was found to be linear to an initial failure load, after which the load-deflection response of the joists then proceeded to behave non-linearly reaching a peak load between 104% and 124% of the initial failure load. According to Thelandersson and Larsen [1], commercial curved timber elements are often susceptible to bending failure initiation due to tension perpendicular to grain stresses. The latticed LVL webs were found to be susceptible to failure in this manner during experimental testing where tensile splitting was observed to emanate from the web at mid-depth of the LVL material along a curved section. Two other failure modes were observed for all joists tested, namely, separation or ‘pop out’ of the LVL web from the flange and separation of the bottom flange from the solid end block close to the support of the I-joist. The geometry of the LVL web was constant for each joist type tested by Harte et al. [14]. The influence of changes to the geometry of the openings is best studied using a numerical approach in the first instance and that is the focus of the present study.

Final Draft

A finite element model is developed and validated against the experimental results presented by Harte et al. [14]. The model is focused on the experimentally determined stiffness and load-displacement response and the failure mechanism at maximum load is not considered. The validated model is utilised to examine the influence of a series of geometric web parameters allowing for an optimised web geometry to be presented.

3 NOVEL LATTICED LVL WEB JOISTS

The I-joists tested by Harte et al. [14], which are the focus of the current work, comprised flanges made from grade C24 Norway Spruce and latticed webs made from LVL. The flange sizes were 50 mm x 60 mm and 55 mm x 65 mm for the 241 mm and 305 mm depths, respectively, as shown in **Fig. 2**. The LVL webs were 31.5 mm x 30 mm and 36 mm x 30 mm for the 241 mm and 305 mm depths, respectively.

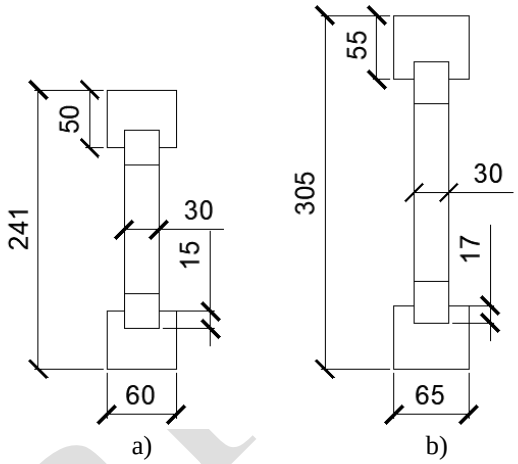

Fig. 2. Section through I-joists, a) 241 mm deep I-joist, b) 305 mm deep I-joist (Dimensions in mm)

LVL is an engineered timber composite manufactured by laminating wood veneers using exterior-type adhesives. In production, veneers are peeled off good quality logs and vertically laminated with successive veneers generally oriented in a common grain direction. This gives LVL its orthotropic properties similar to those in sawn timber [13].

The LVL webs are made up of a number of identical components connected linearly in sequence. In the manufacture of the LVL web components, the veneers (1.8 mm - 2 mm thick) were initially glued flat one on top of the other to form a flat billet. The flat billet is then placed in a radio frequency (RF) press and allowed to cure. The pressed billets were then cut into 30 mm wide sections (**Fig. 3**) each of which is joined by a finger joint in the final joist. In the manufacture of the LVL used in this study, the majority of the billets used Norway Spruce veneers. However, one billet was manufactured using Irish Sitka Spruce and was used in the manufacture of two 241 mm joists.

Final draft

Fig. 3. Manufactured lattice web component with finger joints.

The joint between the lattice LVL web components and the flange is formed by routing a groove in the flanges into which the web is inserted and adhesively bonded. In Harte et al. [14], grooves of 15 mm and 17 mm were routed for the 241 mm and 305 mm deep I-joists, respectively. The routed groove is indicated in **Fig. 4**. For the joists, a solid end section with a minimum length of 185 mm and a maximum length of 250 mm is provided (**Fig. 4**). The minimum length ensures that there is adequate length available for onsite adjustment.

Manufacture of the joists was carried out at the Wood Technology Centre at the University of Limerick. Prior to the manufacture of the joists, all of the flanges and LVL material were subjected to experimental testing to characterise the material. This data is used in the FE model presented here. Joists were tested in four-point bending over a simply supported span of 18 times the joist depth in accordance with the EOTA TR002 standard [29]. This required a span of 4.338 m for the 241 mm deep I-joist and 5.490 m for the 305 mm deep I-joist.

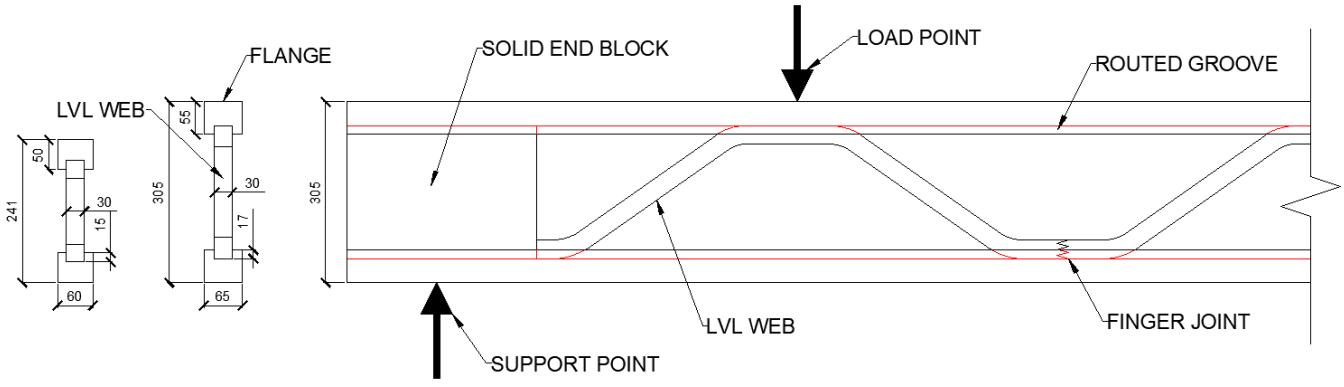

Fig. 4. I-joist cross-section and lattice LVL I-joist components (Harte et al. [14]) (Dimensions in mm)

Draft

4 FINITE ELEMENT MODEL

A three-dimensional FE model of each joist tested by Harte et al. [14] was developed using ANSYS commercial software [30]. The mesh was created using the Solid92 element. This is a 10-node tetrahedral structural solid element with three translational degrees of freedom at each node.

Due to symmetry, it was only necessary to model half the span and half the width of the I-joist. The geometric quarter model is shown in **Fig. 5**. To replicate the experimental test conditions, the vertical component of displacement was set to zero at the support location to simulate a roller condition. In the laboratory tests, the loading was applied through steel plates which were also included in the model. In the FE model, the point load was converted to an equivalent pressure load and applied to the top surface of the steel plate as shown in **Fig. 5**.

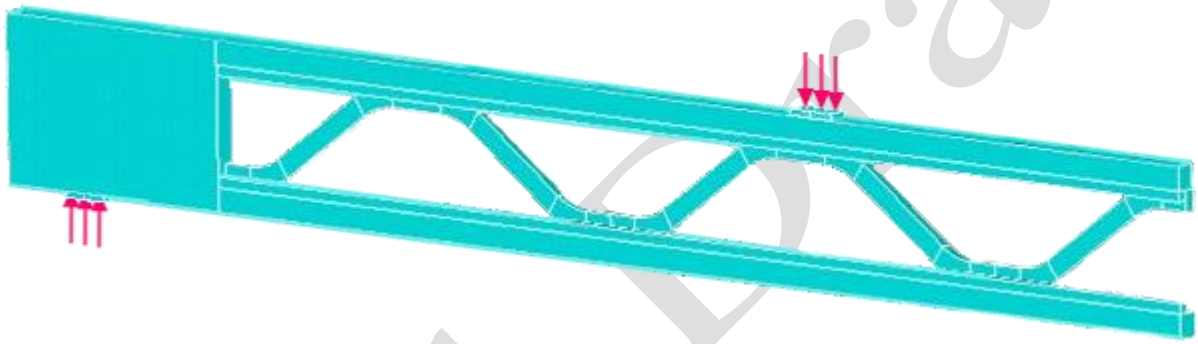

Fig. 5. Geometric FE model of four-point bending test utilising quarter symmetry.

A mesh sensitivity analysis was carried out and it revealed that a mesh element size of 10 mm would adequately model the load-deflection response and the stresses in the web and flange for both sizes of I-joist. A mesh element size of 10 mm requires a total number of elements of approximately 58000 for a typical 241 mm I-joist (12000 in web, 33000 in flanges, 13000 in the solid end section and 250 for the steel plate). **Fig. 6** shows the FE model with the typical initial and final deflected shapes of a 241 mm deep I-joist.

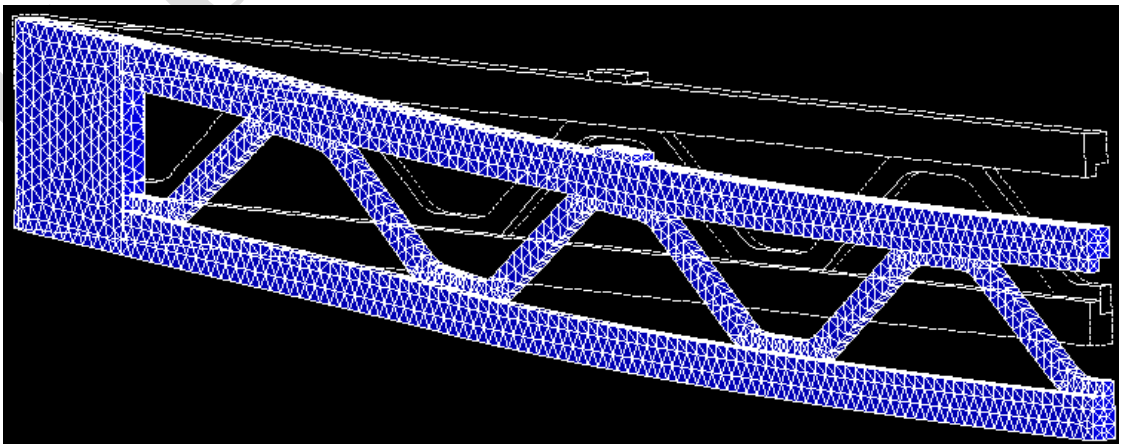

Fig. 6. Initial and final deflected shape of the FE model

Final Draft

4.1 Material Modelling

The LVL web and C24 grade timber flanges were modelled as orthotropic linear elastic materials, while the steel loading plates were modelled using isotropic linear elastic properties. Timber and timber products behave in a linear fashion in tension but in compression timber displays non-linear behaviour. During the testing of the latticed web joists, there was no evidence of compression yielding and the response was linear to failure for 21 of the 24 joists tested so these linear models were deemed satisfactory. Even for linear elastic models, determining the full set of orthotropic material constants for timber and engineered wood products can be challenging but the critical material parameters that influence the structural performance can be determined through a sensitivity study which is discussed further in this section.

4.1.1 *LVL Webs*

As the properties of LVL can vary depending on the lay-up of the product e.g., veneer thickness, glue type and the heat and pressure applied during the manufacturing process, a range of LVL material properties from the literature were used to carry out a FE material sensitivity analysis on a single LVL web component. The range of values for the material properties was taken from Thelandersson and Larsen 2003 [1], Bodig & Jayne [31], Ozelton and Baird [32] and Porteous and Kermani [13]. A vertical load was applied to a model of a single web component, which was supported on roller supports and fixed horizontally on one side. The maximum vertical and horizontal displacements were then calculated. Variation of each material parameter revealed that the elastic modulus in the longitudinal direction (E_x) was the most significant parameter to affect the performance of the component in terms of displacement. As the LVL is susceptible to perpendicular to grain failure in the current application it was also important to ascertain the tensile strength characteristics in this direction. As a result, the elastic modulus parallel to the grain (E_x) and the strength of the LVL material in tension perpendicular to the grain ($f_{t,90}$) were determined experimentally at the Wood Technology Centre at the University of Limerick on samples taken during the production of the LVL lattice webs. These individual LVL material properties were used in the FE model for each joist where possible. The values of the modulus of elasticity for each specimen varied between 10980 and 15155 N/mm^2 and the tension strength perpendicular to the grain ($f_{t,90}$) was found to range between 0.56 – 3.24 N/mm^2 depending on the adhesive used and the timber species.

4.1.2 *Timber flanges*

O'Toole [33] carried out a finite element material sensitivity analysis on similar sized I-joists to those considered in the current study albeit with Sitka Spruce flanges and OSB solid webs. The study revealed that the longitudinal modulus of elasticity (E_x) of the flange was a significant material parameter and greatly influenced the flexural response. For this reason, prior to the manufacture of the joists, all of the flanges were tested non-destructively using a Cook Bolinder machine grader so that the actual modulus of elasticity in the longitudinal direction is known and can be used in the numerical model. The values of the modulus

Final Draft

of elasticity (E_x) for each flange varied between 8225 and 15730 N/mm^2. The other flange stiffness properties, namely the perpendicular to the longitudinal axis (E_y and E_z), the Poisson's ratios and shear moduli in the three orthotropic directions were taken from Bodig & Jayne [31]. The flange strength properties used were the values for C24 timber given in EN 338 [34].

A full list of the material properties of the web and flange material used in the finite element model is given in **Table 1**. For the steel plates, the elastic modulus was taken as 205 N/mm^2 and Poisson's ratio as 0.3. It was assumed that no failure occurred in the glue line between the flange and web and a tied constraint was implemented in the finite element model.

Table 1. Material Properties used for FE analysis.

Material Property	Norway Spruce C24	LVL
E_x (N/mm^2)	8225-15730	10980 – 15155
E_y (N/mm^2)	771	255
E_z (N/mm^2)	407	255
G_{xy} (N/mm^2)	676	380
G_{yz} (N/mm^2)	57	380
G_{xz} (N/mm^2)	636	380
ν_{xy}	0.37	0.22
ν_{yz}	0.47	0.2
ν_{xz}	0.42	0.45

4.2 Geometric Modelling

The complete I-joist geometry can be defined using the following parameters: Top Web Section Length (L_1), Web Inner Radius (R), Web Angle (θ), Web X Section Depth (L_2), Web Width (L_3), Flange Penetration Depth (L_4), Flange Depth (L_5), Flange Width (L_6) and I-Joist Depth (L_7). The Bottom Web Section Length (L_8), Diagonal Web Section Length (L_9), Web Component Length (L_{10}) and the Solid End Length (L_{11}) are dependent geometric parameters. These are illustrated in **Fig. 7** and **Fig. 8**a.

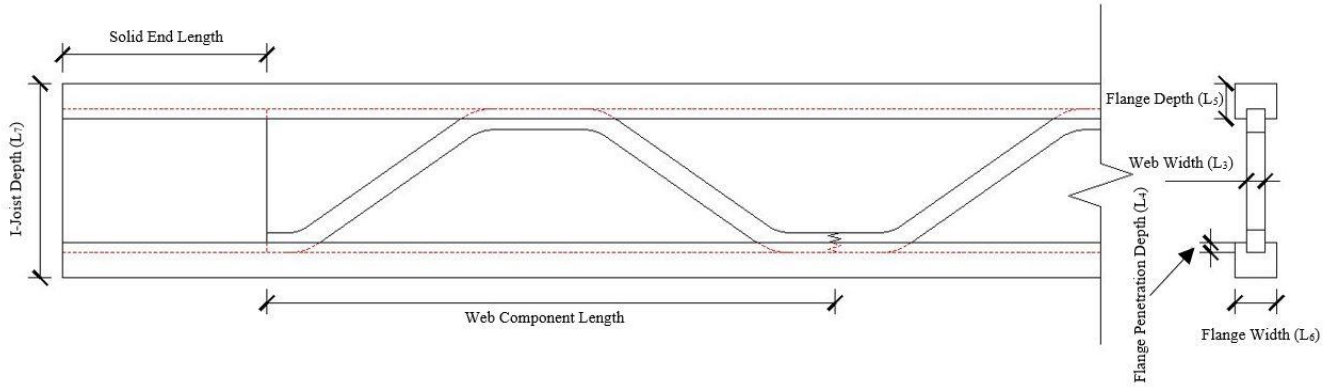

Fig. 7. Longitudinal section and cross-section of latticed webbed I-joist with geometric parameters.

Final Draft

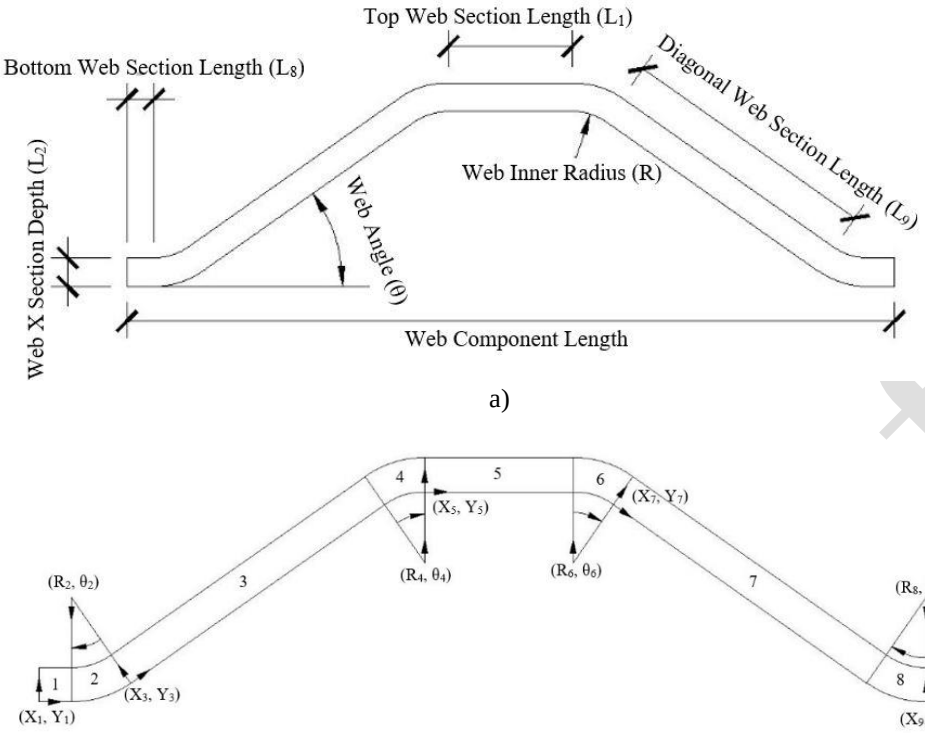

Fig. 8. Lattice web component (a) Geometric parameters (b) Local coordinate systems used for the FE model and the assigned Sections (1-9).

The geometry of each LVL lattice web component is created using 9 separate sections as shown in **Fig. 8**b. Sections 1, 5 and 9 are rectangular and orientated horizontally. Sections 3 and 7 are rectangular and orientated diagonally whilst Sections 2, 4, 6 and 8 are cylindrical. The angle subtended by each cylindrical section is equal to the Web Angle (θ) (**Fig. 8**a). Each of the 9 sections of the web component is assigned a local coordinate system in the model. In ANSYS, the mesh material properties are specified to coincide with the local coordinate system. This ensures the orthotropic material properties of the LVL will follow the orientation of the web component profile as shown in **Fig. 9**a and **Fig. 9**b.

Final Draft

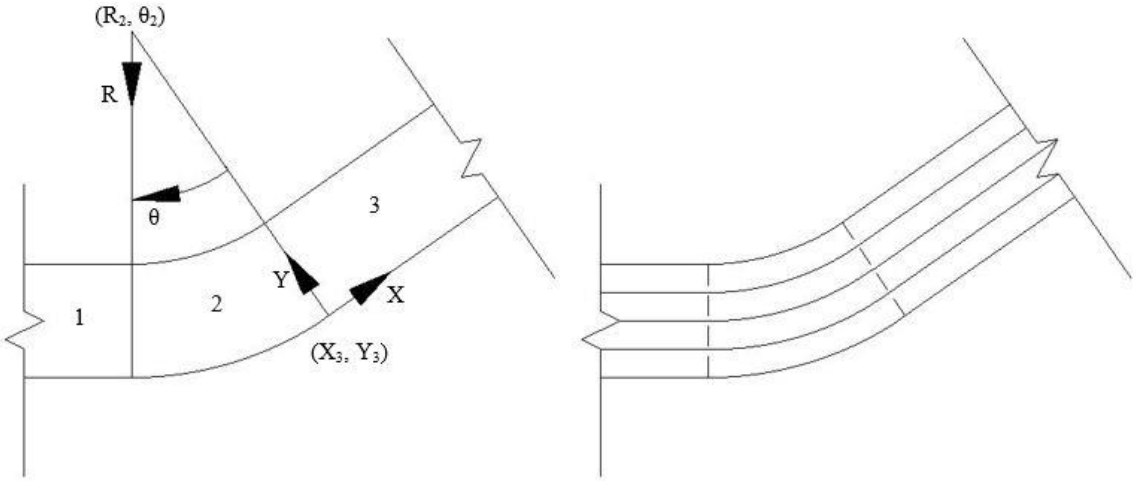

a) b)

Fig. 9. The local coordinate system of the LVL lattice, a) Web Sections 1, 2 and 3 b) modelled orientation of the material.

Once the geometric parameters have been chosen the "Top Web Section Length (L_1)" fixes the "Bottom Web Section Length (L_8)" as shown in Eq. (1).

$$L_1 = L_8 * 2 \tag{1}$$

The parameter "Web Inner Radius (R)" fixes the origin of the cylindrical coordinate system for Section 2. The cylindrical section rotates through "Web Angle (θ)" from the vertical to the beginning of the diagonal web section. The "Diagonal Web Section Length (L_9)" is calculated using Eq. (2).

$$L_9 = L_7 - \big((L_5 - L_4) * 2\big) - (L_2 * 2) - \Big(\big(R - (R * \cos\theta)\big) * 2\Big) + \frac{L_2 * Cos\theta}{Sin\theta} \tag{2}$$

The origin of the cylindrical coordinate system is located using the end of Section 3 and again the "Web Inner Radius (R)" parameter. Section 4 is created by rotating from the end of the diagonal chord clockwise through "Web Angle (θ)" which will end in the vertical position. The Top Web Section Length (L_1) is then added onto this vertical position. The right-hand side of the model is created using the same procedure as for the left-hand side. The total "Web Component Length (L_{10})" is then calculated using Eq. (3).

$$L_{10} = L_1 + \big((R + L_2) * Sin\theta\big) + (R * \sin\theta) + (L_9 * \cos\theta) \tag{3}$$

The "Web Component Length (L_{10})" is then used to calculate the number of components that will fit into the length of the I-joist inclusive of solid end lengths.

Final Draft

5 NUMERICAL RESULTS

5.1 Numerical v Experimental Displacement Response

The physical test data from Harte et al. [14] and corresponding FE predictions are shown in **Table 2** and **Table 3** for the 241 mm and 305 mm I-joists, respectively. In **Table 2** and **Table 3**, $\Delta_{0.4}$ refers to the displacement at 0.4 times the peak load (i.e., the maximum load reached during the test) whereas Δ_{max} refers to the displacement at peak load. The data in the FE columns is the displacement from the results of the FE model at the corresponding test load determined during experimental testing. In **Table 2**, it can be seen that a proportion of the joist used urea-formaldehyde (UF) adhesive in the manufacture of the LVL webs while all other joists used phenol resorcinol formaldehyde (PRF) adhesive. Also, it should be noted that the LVL webs of joists (LVL 13 and LVL 14) 241_7 and 241_8 were manufactured using Irish Spruce lamellae (denoted by * in the Joist ID column) as opposed to Norway Spruce, which was used in all other joists. Although the sample size of joists which uses Irish Spruce is too small to draw any firm conclusions, it is noted that they performed comparatively well in the tests [14]. All of the 305 mm deep I-joists presented in **Table 3** used PRF adhesive.

Table 2. Bending test results for 241 mm deep I-joists

Joist ID	Adhesive	Peak load (kN)	$\Delta_{0.4}$ (mm)		$\frac{\Delta_{0.4,Test}}{\Delta_{0.4,FE}}$	Δ_{max} (mm)		$\frac{\Delta_{max,Test}}{\Delta_{max,FE}}$	$\frac{EI_{Test}}{EI_{FE}}$
			Test	FE		Test	FE		
241_1	UF	6.1	5.3	6.4	0.83	14.3	15.6	0.92	1.23
241_2		5.6	6.2	7.3	0.85	18.8	17.9	1.05	1.15
241_3		6.8	10.2	10	1.02	27.6	24.5	1.13	0.95
241_4		5.9	6.7	7.6	0.88	17.5	18.5	0.95	1.04
241_5		8.0	10.1	10.3	0.98	26.4	25.3	1.04	1.00
241_6		7.6	8.1	9.1	0.89	21.6	22.4	0.96	1.08
241_7*		8.6	9.9	11.6	0.85	26.7	28.6	0.93	1.14
241_8*		9.0	10.8	10.7	1.01	26.9	26.2	1.03	1.04
241_9	PRF	8.7	11.0	12.1	0.91	28.2	29.8	0.95	1.04
241_10		5.2	10.5	7.2	1.46	32.1	17.6	1.82	0.65
241_11		7.9	9.9	10.9	0.91	25.1	26.9	0.93	1.11
241_12		7.2	9.7	9.7	1.00	25.1	23.7	1.06	0.98
241_13		7.3	10.8	9.4	1.15	27.8	23.1	1.20	0.94
241_14		7.7	8.9	9.7	0.92	26.3	23.9	1.10	1.06
241_15		6.8	6.7	7.8	0.86	18.4	19.2	0.96	1.08
241_16		7.8	9.1	9.6	0.95	26.3	23.6	1.11	0.92
Mean	-	7.2	9.0	9.3	0.97	24.3	22.9	1.07	1.03

*LVL webs manufactured using UF glue and Irish Spruce lamellae (otherwise Norway Spruce lamellae used)

As shown in **Table 2**, the displacement at 0.4 times the peak load, $\Delta_{0.4}$ is between 0.83 and 1.46 (1.15 if 241-10 is excluded) the predicted FE model displacement for the equivalent load. At peak load, the displacements are between 0.92 and 1.82 (1.20 if 241-10 is excluded) the predicted FE model displacement for the equivalent load. Joist 241_10 has been specifically mentioned as it resulted in a significantly lower failure load than the other 241 mm deep I-joists. Possible reasons for this were identified

Final Draft

as (1) the solid end block height was too great resulting in tension forces tending to pull the flange away from the web; (2) clamping method used in the manufacture of joists results in an inadequate bond between the flange and web resulting in premature failure [14]. The stiffness ratios (EI_{Test} / EI_{FE}), which correspond to the slope of the load-displacement curve between 0.1 and 0.4 times the peak loads, were between 0.65 (0.92 if 241-10 is excluded) and 1.23. Overall, the FE model results are in good agreement with the experimental results with mean values of the deflection and stiffness ratios close to a value of 1.

Table 3. Bending test results for 305 mm deep I-joists.

Joist ID	Peak load (kN)	$\Delta_{0.4}$ (mm)		$\frac{\Delta_{0.4,Test}}{\Delta_{0.4,FE}}$	Δ_{max} (mm)		$\frac{\Delta_{max,Test}}{\Delta_{max,FE}}$	$\frac{EI_{Test}}{EI_{FE}}$
		Test	FE		Test	FE		
305_1	8.7	9.4	12.1	0.78	29.1	29.7	0.98	1.26
305_2	9.3	10.7	12.7	0.84	33.4	31.0	1.08	1.10
305_3	7.8	9.2	11.7	0.78	26.5	28.6	0.93	1.33
305_4	10.0	12.8	14.1	0.90	40.2	34.4	1.17	0.95
305_5	9.1	12.6	13.1	0.96	33.5	32.1	1.04	1.02
305_6	10.7	13.4	14.9	0.90	37.4	36.6	1.02	1.07
305_7	10.4	11.8	14.2	0.83	33.2	34.9	0.95	1.17
305_8	8.7	10.4	12.1	0.86	30.6	29.5	1.04	1.12
Mean	9.3	11.3	13.1	0.86	33.0	32.1	1.03	1.13

As shown in **Table 3**, when examining joist depths of 305 mm, the displacement at 0.4 times the peak load, $\Delta_{0.4}$ is between 0.78 and 0.96 times those of the predicted FE model displacement for the equivalent load. At peak load, the FE model predicted displacements of between 0.93 and 1.17 times that of the experimental test. The stiffness ratios (EI_{Test} / EI_{FE}) were found to be in the range between 0.95 and 1.33 indicating a good correlation between the experimental and FE model results. **Fig. 10** and **Fig. 11** show the load-displacement test results and FE model predictions for representative 241 mm and 305 mm deep joists, respectively. As can be observed, there is a good correlation between the experimental test data and the FE results up until the peak load.

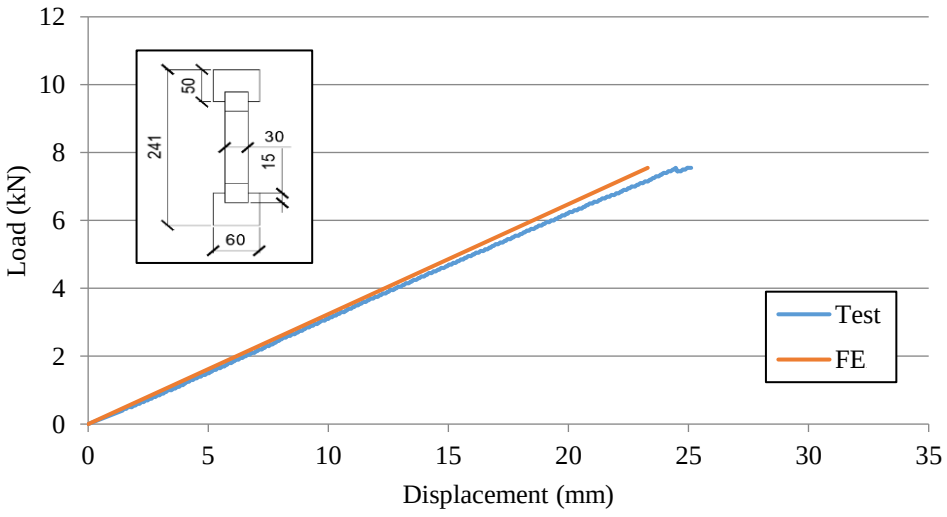

Fig. 10. Load-displacement behaviour of experimental tests against FE results for I-joist 241_12

Final Draft

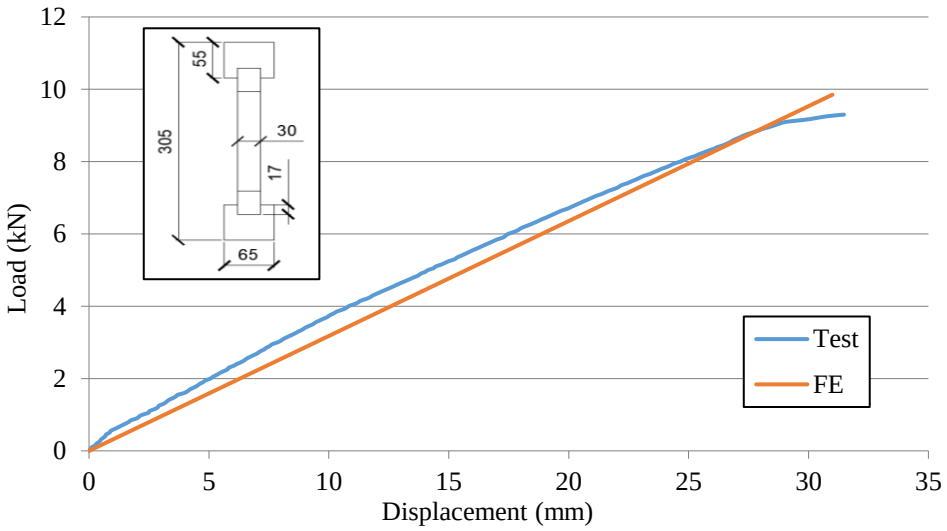

Fig. 11. Load-displacement behaviour of experimental tests against FE results for I-joist 305_2

5.1 Numerical Stress Results

Three distinct failure modes were observed during experimental testing: i) tensile splitting perpendicular to the grain in the LVL web (T), ii) pop-out of the 1st LVL web component from the top or bottom flange groove (P), and iii) separation of the solid end block from the bottom flange (S). Examples of these failure modes are illustrated in Harte et al. [14]. Whenever failure mode iii) occurred, it always did so subsequent to failure modes i) or ii) occurring. Failure mode iii) is not investigated here using the FE model. **Table 4** and **Table 5** present the stress perpendicular to the grain in the web ($\sigma_{t,90,max}$) as determined from the FE model, the experimentally determined tensile strength perpendicular to the grain ($f_{t,90}$) along with the associated failure modes for the 241 mm and 305 mm deep joists, respectively. In order to maintain consistency with the notation used in Harte et al. [14], failure modes i) and ii) are denoted by T and P, respectively, in the failure mode column of **Table 4** and **Table 5**. In **Table 4** and **Table 5**, $\sigma_{t,90,max}$ corresponds to the maximum stress perpendicular to the grain in the LVL web from the FE model results corresponding to the maximum load observed experimentally. Additionally, when available, $f_{t,90}$ is presented which corresponds to the characteristic tensile strength perpendicular to the grain for the LVL web as determined from experimental tests on additional LVL samples manufactured from the same billet.

Table 4. Numerical stress results and failure modes for 241 mm deep I-joists

Joist ID	Adhesive	LVL Web		Failure mode
		$\sigma_{t,90,max}$ (FE) N/mm^2	$f_{t,90}$ (Exp) N/mm^2	
241_1		1.09	NA	T
241_2		1.23	NA	T
241_3		1.47	1.21	T
241_4	UF	1.21	1.21	P
241_5		1.62	0.56	T
241_6		1.54	1.21	T
241_7*		1.89	3.24	P

Final Draft

241_8*		2.04	3.24	P
241_9	PRF	1.89	NA	P
241_10		1.20	3.24	P
241_11		1.70	NA	P
241_12		1.54	1.14	P
241_13		1.67	0.56	P
241_14		1.66	0.56	P
241_15		1.36	NA	T
241_16		1.58	NA	P
Mean		1.54	1.62	-

* = LVL webs manufactured using UF glue and Irish Spruce lamellae (otherwise Norway Spruce lamellae used)

Failure of the 241 mm deep I-joists with Norway Spruce veneers and UF glue was due to tension failure perpendicular to the grain in the webs for all joists except I-joist 241_4 which failed due to a separation of the web from the top flange (P). For all the other UF joists with available $f_{t,90}$ data, the LVL tensile stress perpendicular to the grain determined by the FE model have surpassed the characteristic strength. **Fig. 12** shows an example of the normal stress distribution perpendicular to the grain in the web for joist 241_6 at peak load. It is noted that $\sigma_{t,90,max}$ is 1.54 N/mm^2 whereas $f_{t,90}$ is 1.21 N/mm^2 for this joist. This particular joist failed due to tensile splitting perpendicular to the grain in the LVL web in experimental tests. This result indicates that the numerical model can be further enhanced to include failure criteria to accurately characterise the post-failure behaviour.

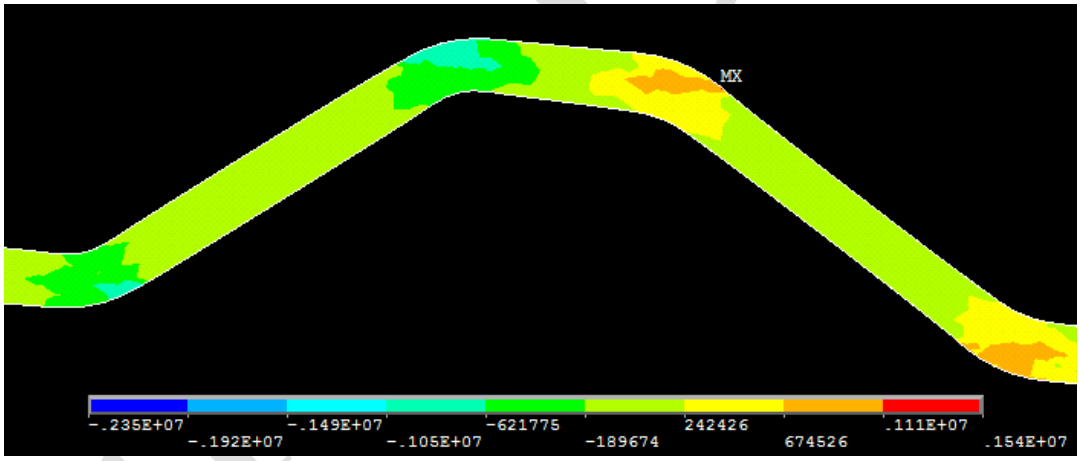

Fig. 12. Normal stress perpendicular to grain at failure load for I-joist 241_6 (N/m^2)

Failure of the 241mm deep I-joists with PRF glue was found to occur due to both tensile splitting perpendicular to the grain of the web and separation of the web from the top or bottom flanges. The results are generally as expected, except for one of the PRF joists which failed due to 'web pop out' of the flange and for which $f_{t,90}$ data is available (I-joist 241_12). For this I-joist, the LVL tensile stress perpendicular to the grain is greater than the characteristic strength and it would be expected that this joist should have failed due to tensile splitting perpendicular to the grain of the web. The remaining joists utilising PRF adhesive, for which there is available $f_{t,90}$ data, failed due to tension failure (T) as expected due to the low strength perpendicular to the grain ($f_{t,90}$) determined from experimental tests. Failure of the 241 mm deep I-joists with Irish Sitka Spruce veneers and UF glue was due to the separation of the web from the flange. For these two joists $\sigma_{t,90,max}$ at peak load is less than $f_{t,90}$ as expected.

Final Draft

Table 5. Numerical stress results and failure modes for the 305 mm deep I-joists

Joist ID	LVL Web		Failure mode
	$\sigma_{t,90,max}$ (FE)	$f_{t,90}$ (Exp)	
	N/mm^2	N/mm^2	
305_1	1.96	2.44	T
305_2	2.07	2.44	P
305_3	1.84	2.44	P
305_4	2.14	2.44	P
305_5	2.04	2.44	P
305_6	2.36	2.44	P
305_7	2.30	2.44	P
305_8	1.88	2.44	P
Mean	2.07	2.44	-

Failure of the 305 joists, all of which used PRF glue, was due to separation of the web from the top or bottom flanges for all joists except for joist 305_1 which failed due to tension failure perpendicular to the grain in the web. For all 305 mm deep joists $\sigma_{t,90,max}$ is less than the mean value of $f_{t,90}$ including joist 305_1 even though its failure was mode i) during experimental testing. The experimental $f_{t,90}$ value of 2.44 N/mm^2 was determined from a series of test specimens manufactured from the same billet used in all 305 mm deep I-joists. Overall, the result of the 305 mm deep I-joists are well characterised by the FE model but there is potential to further enhanced and include failure criteria to accurately characterise the post-failure behaviour.

6 FE GEOMETRY OPTIMISATION

A FE investigation was carried out to determine if the structural performance of the I-joists could be improved by varying the geometric parameters of the LVL web component. The aim was to maximise the stiffness whilst minimising the stress perpendicular to the grain in the LVL webs and the shear stresses at the web/flange interface. The material properties used in this parameter study were as in **Table 1** with individual flange material properties taken from I-joist 241_12 ($E_{x,\text{ top flange}}$ = 8991 N/mm^2 and $E_{x,\text{ bottom flange}}$ = 10150 N/mm^2) and I-joist 305_2 ($E_{x,\text{ top flange}}$ = 15730 N/mm^2 and $E_{x,\text{ bottom flange}}$ = 14842 N/mm^2). For both I-joist sizes, the individual web material properties were taken from the best performing LVL billet, which used Norway Spruce lamellae and PRF glue i.e. $E_{x,LVL}$ = 13056 N/mm^2. The same LVL material was shown to have a mean tensile strength perpendicular to the grain ($f_{t,90,LVL}$) of 2.44 N/mm^2.

For the 241 mm deep I-joist, the following geometric parameters previously presented in **Fig. 8** were fixed: Web X Section Depth (L_2) = 31.5 mm, Flange Depth (L_5) = 50 mm, and Flange Width (L_6) = 60 mm. The Top Web Section Length (L_1), Web Width (L_3), Flange Penetration Depth (L_4), Web Angle (θ), and Web Inner Radius (R), were then varied (**Fig. 8**). The ranges considered for each geometric parameter along with the final optimum values for the 241 mm deep joists are shown in **Table 6**.

In the consideration of various designs, it is necessary to adhere to a number of geometric constraints. The Diagonal Web Section Length (L_9) must have a positive value, the Web Component Length (L_{10}) must be less than 750 mm and the range for the Solid End Length (L_{11}) must lie between 185 mm and 250 mm the reasons for which were previously outlined. Additionally,

Final Draft

a 70 mm minimum limit was placed on the outer fillet radius. This was a manufacturing constraint below which the veneers of the LVL would split due to the tightness of the curve. This corresponds to a minimum value for the Web Inner Radius (R) (70 mm – Web X Section Depth (L_2)) which corresponds to 34 mm and 38.5 mm for the 241 mm deep and 305 mm deep I-joists, respectively.

Some of the minimum and maximum values considered for each variable are dependent on the values of the other variables. For example, the limits on the ranges for the Web Inner Radius (R) and the Top Web Section Length (L_1) are co-dependent. If the value of the Web Inner Radius (R) is chosen at the upper limit of its range, it would require the value of the Top Web Section Length (L_1) to be at the lower limit of its range to facilitate the Web Component Length (L_{10}) adhering to its 750 mm maximum length.

Following the FE investigation of the full range of possible 241 mm deep I-joist designs, Δ_{max} varied between 23.7 mm and 65.7 mm, $\sigma_{t,90,max,LVL}$ varied between 1.11 N/mm^2 and 6.12 N/mm^2, at the web/flange interface, $\tau_{max,flange}$ varied between 2.92 N/mm^2 and 9.26 N/mm^2 and $\tau_{max,web}$ varied between 4.93 N/mm^2 and 12.5 N/mm^2, $\sigma_{0,bottom\ flange}$ varied between 12.8 N/mm^2 and 25.0 N/mm^2 and the Web Component Length (L_{10}) varied between 306 mm and 737 mm.

Table 6. Details of optimisation for 241 mm and 305 mm I-joists

Geometric Parameter	Dependent or Independent Parameter	Range	Optimum 241 mm I-Joist	Optimum 305 mm I-Joist
I-Joist Depth (L_7)	Independent	Fixed	241mm	305 mm
Flange Depth (L_5)	Independent	Fixed	50 mm	55 mm
Flange Width (L_6)	Independent	Fixed	60 mm	65 mm
Web X Section Depth (L_2)	Independent	Fixed	31.5 mm	36 mm
Web Angle (θ)	Independent	15° – 90°	35°	40°
Flange Penetration Depth (L_4)	Independent	10 mm – 20 mm	15 mm	17 mm
Web Inner Radius (R)	Independent	34 or 38.5 mm – 175 mm	55 mm	50 mm
Web Width (L_3)	Independent	10 mm – 40 mm	30 mm	30mm
Top Web Section Length (L_1)	Independent	20 mm – 100 mm	85 mm	90 mm
Diagonal Web Section Length (L_9)	Dependent	Min 0 mm	198 mm	235 mm
Web Component Length (L_{10})	Dependent	Max 750 mm	658 mm	715 mm
Solid End Length (L_{11})	Dependent	185 mm – 250 mm	196mm	243 mm

For the optimum 241 mm deep I-joist design presented in **Table 6**, Δ_{max} was 23.7 mm, $\sigma_{t,90,max,LVL}$ was 1.54 N/mm^2, at the web/flange interface $\tau_{max,flange}$ was 5.77 N/mm^2 and $\tau_{max,web}$ was 4.93 N/mm^2, and $\sigma_{0,bottom\ flange}$ was 12.8 N/mm^2. At 658 mm, although the Web Component Length (L_{10}) for the optimum design is over twice as long as some of the designs considered, it performed significantly better than the shorter designs. This increased length provides a significant benefit in terms of space for positioning of services through the web but also reduces the flexibility in terms of varying the span as the total span of the I-Joist comprises the sum of the total number of latticed LVL web components plus the solid end length at the supports.

The stiffness of the joist was found to be primarily affected by the Web Angle (θ), the bond area at the web/flange interface was affected by the Flange Penetration Depth (L4) and the Top Web Section Length (L1) and the stress perpendicular to the

Final Draft

grain in the web at the curved LVL sections were affected by the Web Inner Radius (R). It was necessary to obtain a balance between each of these parameters as there is a trade-off amongst them as outlined below in **Fig. 13** and **Fig. 14**. The optimum Web Angle (θ) value of 35°corresponds to the stiffest design. When the normal stresses are analysed (i.e., the stresses parallel to the LVL grain) it can be observed that at an angle of 35°, the diagonal section of the web component acts more like a strut or truss member. This can be observed in **Fig. 13** where there are predominant compressive stresses on the left diagonal section and predominant tensile stresses on the right diagonal section. This contrasts with the bending behaviour of the diagonal section for a 70° Web Angle (θ) seen in **Fig. 14**. This can be observed in **Fig. 14** where there are both tensile and compressive stresses on each diagonal section.

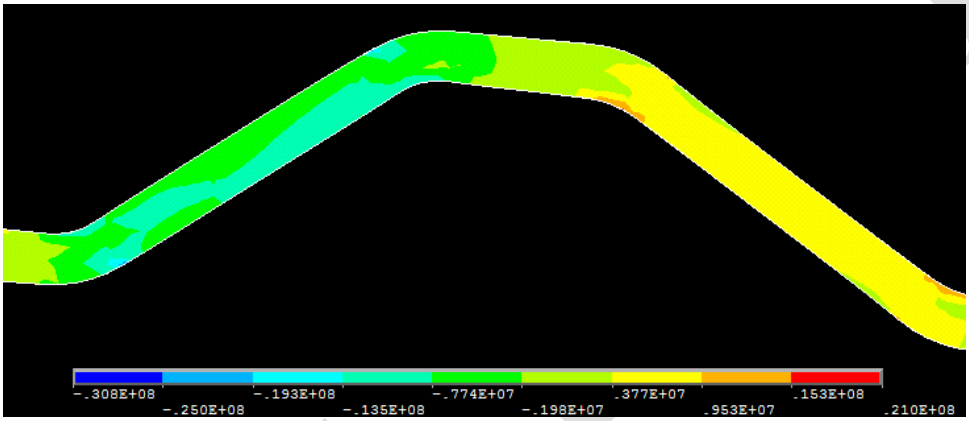

Fig. 13. Normal stresses (N/m^2) in the web parallel to LVL grain for 35° Web Angle (θ). The left diagonal arm is in compression (-negative) whilst the right diagonal arm is in tension (+positive).

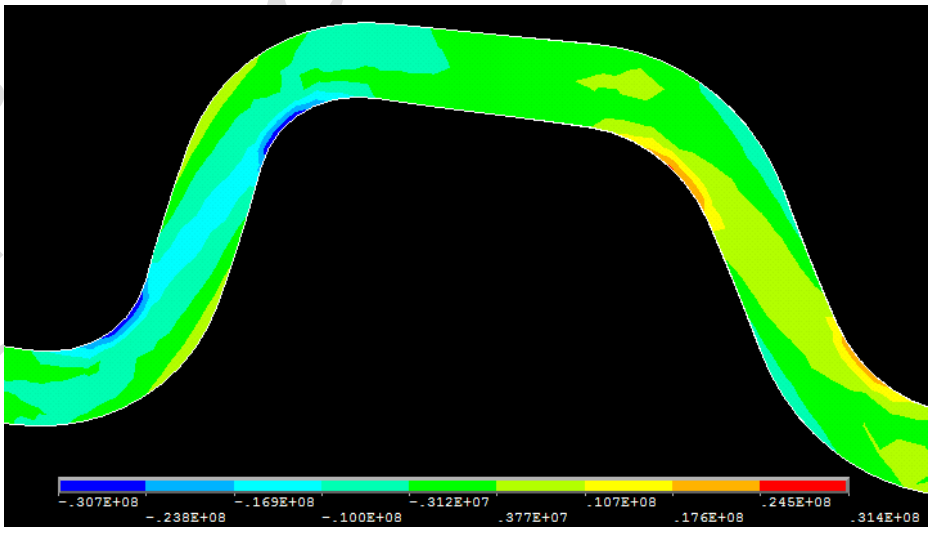

Fig. 14. Normal stresses (N/m^2) in the web parallel to the LVL grain for a 70° Web Angle (θ). There are both compressive (-negative) and tensile (+positive) stresses on each diagonal arm.

Final

An increase of the Web Angle (θ) above 35° also resulted in a larger midspan deflection. A decrease of this angle resulted in the Web Component Length (L_{10}) exceeding its limit unless a very small Top Web Section Length (L_1) was used. The effect of the Top Web Section Length (L_1) and the Web Inner Radius (R) was found to have an insignificant effect on deflection but if a small Top Web Section Length (L_1) was used, the shear stresses would increase at the web/flange interface. In analysing shear at the web/flange interface it was observed that, for a 35° Web Angle (θ), reducing the Top Web Section Length (L_1) from 85 mm to 20 mm increased shear stress at the flange ($\tau_{max,flange}$) from 5.77 to 9.26 N/mm^2. An optimum value of 85 mm for the Top Web Section Length (L_1) is specified to ensure an adequate bond length at the web/flange interface.

For a 35° Web Angle (θ) and a Top Web Section Length (L_1) of 85 mm, varying the Flange Penetration Depth (L_4) between 10 and 20 mm only had a minor effect on the shear stresses at the web/flange interface. The optimum values for the Flange Penetration Depth (L_4) and the Web Width (L_3) were 15 mm and 30 mm, respectively. Decreasing these values led to minor increases in deflection.

For the 305 mm deep I-joist the following geometric parameters were fixed: Web X Section Depth (L_2) = 36 mm, Flange Depth (L_5) = 55 mm, and Flange Width (L_6) = 65 mm. The Top Web Section Length (L_1), Web Width (L_3), Flange Penetration Depth (L_4), Web Angle (θ), and Web Inner Radius (R), were then varied. The ranges considered for each geometric parameter along with the final optimum values for the 305 mm deep I-joist are also shown in **Table 6**.

Following the FE investigation of a series of possible 305mm deep I-joist designs, Δ_{max} varied between 21.4 mm and 87.0 mm, $\sigma_{t,90,max,LVL}$ varied between 1.11 N/mm^2 and 6.12 N/mm^2, at the web/flange interface $\tau_{max,flange}$ varied between 2.92 N/mm^2 and 9.26 N/mm^2 and $\tau_{max,web}$ varied between 4.93 N/mm^2 and 12.5 N/mm^2, $\sigma_{0,bottom\ flange}$ varied between 12.8 N/mm^2 and 34.3 N/mm^2 and the Web Component Length (L_{10}) varied between 306 mm and 737 mm.

For the optimum 305 mm deep I-joist design, Δ_{max} was 25.2 mm, $\sigma_{t,90,max,LVL}$ was 1.81 N/mm^2, at the web/flange interface $\tau_{max,flange}$ was 5.14 N/mm^2 and $\tau_{max,web}$ was 1.24 N/mm^2, $\sigma_{0,bottom\ flange}$ was 18.0 N/mm^2. Although some designs displayed stiffer results, they also had a smaller Web Angle (θ) which required a very small Top Web Section Length (L_1). The key changes for the 305 mm I-joist over the 241 mm depth are as follows:

- An increase in the Web Angle (θ) from 35° to 40°. This was necessary due to the maximum restriction on the Web Component Length (L_{10}) whilst also specifying an adequate Top Web Section Length (L_1).
- An increase in the Top Web Section Length (L_1) from 85 mm to 90 mm and an increase in the Flange Penetration Depth (L_4) from 15 mm to 17 mm. Both of these changes will increase the bond area for each component. These changes had a negligible effect on stiffness.

Final Draft

- An increase in the Web X Section Depth (L_2) from 31.5 mm to 36 mm. Although the stresses perpendicular to the grain in the LVL were not high, this increase is recommended to facilitate easier manufacture of the final web component from the billet. The effect the increase in web depth had on stiffness was negligible.

7 SUMMARY AND CONCLUSIONS

Two composite timber I-joists with Norway Spruce flanges and latticed LVL webs have been modelled and analysed using the finite element method. The component materials were modelled as linear orthotropic elastic materials in both tension and compression. The developed model has been shown to predict the behaviour of the novel latticed LVL webbed I-joist reasonably well with good correlation between the FE model and physical test data for sixteen 241 mm deep I-joists and eight 305 mm deep I-joists. The model has been shown to adequately predict the elastic stiffness and vertical displacement behaviour of this novel product. The validated model provides a useful tool for further FE investigations into the structural response of this product and has been used as part of a parameter study to optimise the design of the latticed LVL webbed elements. The FE parameter study was carried out on each I-joist size to determine the optimum design of the web component geometry to maximise stiffness whilst minimising the stress perpendicular to the grain of the LVL. The optimum designs have been presented. Further studies are required to firstly, experimentally confirm the findings from the optimised design presented herein and secondly, to further develop the FE model to incorporate failure criteria to predict the failure behaviour of such elements.

CONFLICT OF INTEREST

The authors confirm that this article's content has no conflict of interest.

ACKNOWLEDGMENT

This work has been carried out as part of the project entitled “Innovative I-Joist Products” (Project Code IP-2007-0453) funded by Enterprise Ireland and Grainger Sawmills under the Innovation Partnership program. The contribution of the technical staff of the College of Engineering and Informatics, NUI Galway, in particular, Peter Fahy, Colm Walsh and Gerard Hynes, is acknowledged. The authors would also like to acknowledge the contribution of project partners, Sean Moloney and Michael Bourke at the Wood Technology Centre, University of Limerick.

NOTATION

x = direction parallel to joist span

y = direction parallel to joist depth

z = direction parallel to joist thickness

E_x = modulus of elasticity in x direction

Final Draft

E_y = modulus of elasticity in y direction

E_z = modulus of elasticity in z direction

G_{xy} = shear modulus in x-y direction

G_{yz} = shear modulus in y-z direction

G_{xz} = shear modulus in x-z direction

ν_{xy} = Poisson's ratio in x-y direction

ν_{yz} = Poisson's ratio in y-z direction

ν_{xz} = Poisson's ratio in x-z direction

$\sigma_{0,max}$ = maximum tensile stress parallel to grain

$\sigma_{t,90,max}$ = maximum tensile stress perpendicular to grain

$f_{t,90}$ = tensile strength perpendicular to grain

τ_{max} = maximum shear stress

L_1 = Top Web Section Length

R = Web Inner Radius

θ = Web Angle

L_2 = Web X Section Depth

L_3 = Web Width

L_4 = Flange Penetration Depth

L_5 = Flange Depth

L_6 = Flange Width

L_7 = I-joist Depth

L_8 = Bottom Web Section Length

L_9 = Diagonal Web Section Length

L_{10} = Web Component Length

L_{11} = Solid End Length

EI_{Test}/EI_{FE} = stiffness ratios obtained from test and FE data

$\Delta_{0.4}$ = displacement at 0.4 times the test peak load

Δ_{max} = maximum displacement

Final Draft

REFERENCES

[1] Thelandersson S, Larsen HJ. Timber Engineering. John Willey & Sons Ltd; 2003.

[2] Leichti RJ, Falk RH, Laufenberg T. Prefabricated Wood Composite I-Beams: A Literature Review. Wood Fiber Sci 1990;22:62–79.

[3] Bahadori-Jahromi A, Kermani A, Zhang B, Reid D. A Parametric Evaluation of Multi-Webbed Composite Joists Based on EC5. J Inst Wood Sci 2007;17:295–310. doi:10.1179/wsc.2007.17.6.295.

[4] Ramage MH, Burridge H, Busse-Wicher M, Fereday G, Reynolds T, Shah DU, et al. The wood from the trees: The use of timber in construction. Renew Sustain Energy Rev 2017;68:333–59. doi:10.1016/j.rser.2016.09.107.

[5] Tang Z, Shan B, Li WG, Peng Q, Xiao Y. Structural behavior of glubam I-joists. Constr Build Mater 2019;224:292–305. doi:10.1016/j.conbuildmat.2019.07.082.

[6] Ghanbari-Ghazijahani T, Russo T, Valipour HR. Lightweight timber I-beams reinforced by composite materials. Compos Struct 2020;233:111579. doi:10.1016/j.compstruct.2019.111579.

[7] Blyberg L, Lang M, Lundstedt K, Schander M, Serrano E, Silfverhielm M, et al. Glass, timber and adhesive joints - Innovative load bearing building components. Constr Build Mater 2014;55:470–8. doi:10.1016/j.conbuildmat.2014.01.045.

[8] Zhu EC, Guan ZW, Rodd PD, Pope DJ. Finite element modelling of OSB webbed timber I-beams with interactions between openings. Adv Eng Softw 2005;36:797–805. doi:10.1016/j.advengsoft.2005.03.027.

[9] Afzal MT, Lai S, Chui YH, Pirzada G. Experimental evaluation of wood I-joists with web holes. For Prod J 2006;56:26–30.

[10] Pirzada GB, Chui YH, Lai S. Predicting Strength of Wood I-Joist with a Circular Web Hole. J Struct Eng 2008;134:1229–34. doi:10.1061/(ASCE)0733-9445(2008)134:7(1229).

[11] Morrissey GC, Dinehart DW, Dunn WG. Wood I-Joists with Excessive Web Openings: An Experimental and Analytical Investigation. J Struct Eng 2009;135:655–65. doi:10.1061/(Asce)St.1943-541x.0000013.

[12] Steensels R, Vandoren B. Experimental and Numerical Analysis of Timber I-Joists with Cut-Outs. Proceedings 2018;2:463. doi:10.3390/icem18-05375.

[13] Porteous J, Kermani A. Structural timber design to Eurocode 5. 2007. doi:10.1017/CBO9781107415324.004.

[14] Harte AM, Baylor G, O'Ceallaigh C. Evaluation of the Mechanical Behaviour of Novel Latticed LVL-Webbed Joists.

Final Draft

Open Constr Build Technol J 2019;13:1–11. doi:10.2174/1874836801913010001.

[15] Liu TCH, Chung KF. Steel beams with large web openings of various shapes and sizes: Finite element investigation. J Constr Steel Res 2003;59:1159–76. doi:10.1016/S0143-974X(03)00030-0.

[16] Kerdal D, Nethercot DA. Failure modes for castellated beams. J Constr Steel Res 1984;4:295–315. doi:10.1016/0143-974X(84)90004-X.

[17] Mohebkhah A, Showkati H. Bracing requirements for inelastic castellated beams. J Constr Steel Res 2005;61:1373–86. doi:10.1016/j.jcsr.2005.03.003.

[18] Kohnehpooshi O, Showkati H. Numerical modeling and structural behavior of elastic castellated section. Eur J Sci Res 2009;31:306–18.

[19] Wang P, Guo K, Liu M, Zhang L. Shear buckling strengths of web-posts in a castellated steel beam with hexagonal web openings. J Constr Steel Res 2016;121:173–84. doi:10.1016/j.jcsr.2016.02.012.

[20] Chung KF, Liu TCH, Ko ACH. Investigation on vierendeel mechanism in steel beams with circular web openings. J Constr Steel Res 2001;57:467–90. doi:10.1016/S0143-974X(00)00035-3.

[21] Mahendran M, Keerthan P. Experimental studies of the shear behavior and strength of LiteSteel beams with stiffened web openings. Eng Struct 2013;49:840–54. doi:10.1016/j.engstruct.2012.12.007.

[22] Jahromi AB, Zhang B, Harte A, Walford B, Bayne K, Turner J. Investigating the structural performance of multi-webs I-Beams. J Inst Wood Sci 2006;17:148–58. doi:10.1179/wsc.2006.17.3.148.

[23] Baylor G, Harte AM. Finite element modelling of castellated timber I-joists. Constr Build Mater 2013;47. doi:10.1016/j.conbuildmat.2013.05.076.

[24] Islam MS, Shahnewaz M, Alam MS. Structural capacity of timber I-joist with flange notch: Experimental evaluation. Constr Build Mater 2015;79:290–300. doi:10.1016/j.conbuildmat.2015.01.017.

[25] Shahnewaz M, Islam MS, Ahmadipour M, Tannert T, Alam MS. Reinforced Wood I-Joists with Web Openings. J Struct Eng 2017;143:04017022. doi:10.1061/(ASCE)ST.1943-541X.0001747.

[26] Zhu EC, Guan ZW, Pope DJ, Rodd PD. Effect of Openings on Oriented Strand Board Webbed Wood I-Joists. J Struct Eng 2007;133:145–9. doi:10.1061/(asce)0733-9445(2007)133:1(145).

[27] Guan Z, Gendall J. Finite element modelling of buckling behaviour of steel webbed timber joists. 10th World Conf Timber Eng 2008 2008;4:2001–8.

Final Draft

[28] Shahidul Islam M, Shahnewaz M, Alam MS. Glass fiber reinforced Polymer (GFRP) retrofitting of timber I-Joists with opening and notch. Structures 2021;34:804–26. doi:10.1016/j.istruc.2021.08.033.

[29] EOTA. Technical Report 002: Test methods for light composite wood-based beams and columns. European Organisation of Technical Approvals; 2000.

[30] ANSYS Inc. ANSYS Documentation: Release 12. 2009.

[31] Bodig J, Jayne BA. Mechanics of Wood Composites. Reprinted edition. Kreiger Publishing Company. USA; 1993.

[32] Ozelton EC, Baird JA. Timber Designers' Manual. Oxford, UK: Blackwell Science Ltd; 2006. doi:10.1002/9780470691021.

[33] O'Toole C. An investigation into the use of Irish Sitka Spruce in timber I-joists. MEngSc thesis, Civil Engineering, National University of Ireland Galway, Ireland, 2006.

[34] CEN. EN 338. Structural timber - Strength classes. Comité Européen de Normalisation, Brussels, Belgium; 2016.

Final Draft